MOLECULAR AND CELLULAR BIOLOGY, Dec. 2007, p. 8683–8697 Vol. 27, No. 24
0270-7306/07/$08.00+0 doi:10.1128/MCB.00157-07

The Nuclear RhoA Exchange Factor Net1 Interacts with Proteins of the Dlg Family, Affects Their Localization, and Influences Their Tumor Suppressor Activity▽†

Rafael García-Mata,[1]* Adi D. Dubash,[1] Lisa Sharek,[1] Heather S. Carr,[2] Jeffrey A. Frost,[2] and Keith Burridge[1]

Department of Cell and Developmental Biology and Lineberger Comprehensive Cancer Center, University of North Carolina at Chapel Hill, Chapel Hill, North Carolina,[1] and Department of Integrative Biology and Pharmacology, University of Texas Health Science Center at Houston, Houston, Texas[2]

Received 26 January 2007/Returned for modification 5 March 2007/Accepted 1 October 2007

Net1 is a RhoA-specific guanine nucleotide exchange factor which localizes to the nucleus at steady state. A deletion in its N terminus redistributes the protein to the cytosol, where it activates RhoA and can promote transformation. Net1 contains a PDZ-binding motif at the C terminus which is essential for its transformation properties. Here, we found that Net1 interacts through its PDZ-binding motif with tumor suppressor proteins of the Dlg family, including Dlg1/SAP97, SAP102, and PSD95. The interaction between Net1 and its PDZ partners promotes the translocation of the PDZ proteins to nuclear subdomains associated with PML bodies. Interestingly, the oncogenic mutant of Net1 is unable to shuttle the PDZ proteins to the nucleus, although these proteins still associate as clusters in the cytosol. Our results suggest that the ability of oncogenic Net1 to transform cells may be in part related to its ability to sequester tumor suppressor proteins like Dlg1 in the cytosol, thereby interfering with their normal cellular function. In agreement with this, the transformation potential of oncogenic Net1 is reduced when it is coexpressed with Dlg1 or SAP102. Together, our results suggest that the interaction between Net1 and Dlg1 may contribute to the mechanism of Net1-mediated transformation.

The Rho family of small GTPases represents a major branch of the Ras superfamily and consists of 22 distinct genes, with RhoA, Rac1, and Cdc42 being the most intensely studied and best characterized family members (67). Rho GTPases control many aspects of cell behavior, such as the organization of the cytoskeleton, cell migration, cell-cell and cell-matrix adhesion, cell cycle progression, gene expression, and cell polarity (7, 24, 65).

Like all GTPases, Rho proteins act as molecular switches by cycling between an active (GTP-bound) and an inactive (GDP-bound) state. Active GTPases interact with high affinity with one of several downstream effectors to modulate their activity and localization. The activation of Rho GTPases is regulated by specific guanine nucleotide exchange factors (GEFs), which catalyze the exchange of GDP for GTP. Signaling is terminated when GTP is hydrolyzed to GDP, a process stimulated by GTPase-activating proteins. In addition, a third family of proteins, the guanine nucleotide dissociation inhibitors, negatively regulate Rho GTPases by sequestering them in the cytoplasm and interfering with both the GDP/GTP exchange and the GTP hydrolysis (65).

More than 70 Rho GEFs and 70 Rho GTPase-activating proteins are encoded by the human genome, allowing for pathway-specific regulation of Rho protein activity (51, 62). In addition, Rho GTPases interact with a wide variety of effectors and act as key players at the crossroads of signal integration and transduction (7, 24, 65).

Rho GEFs comprise a highly diverse family of proteins that share a common catalytic domain (Dbl homology [DH]), followed by a Pleckstrin homology (PH) domain, but are very different otherwise in their domain structures (51, 54). A striking feature of Rho GEFs is that they outnumber their target GTPases by a factor of 3, which means that multiple GEFs are capable of activating the same GTPase. In addition, many GEFs can activate more than one GTPase (51, 54). One of the fundamental questions in the field is how a cell utilizes specific combinations of GEF, GTPase, and effector to elicit defined responses to specific extracellular stimuli.

We have recently shown that 26 out of 70 Rho GEFs of the human DH family (37%) contain a putative PDZ-binding motif at the C terminus (18). These binding motifs are present in almost all of the corresponding mouse homologs, suggesting an evolutionarily conserved role. PDZ domains are protein-protein interaction domains that act as scaffolds to concentrate signaling molecules at specialized regions in the cell. In recent years, a series of PDZ proteins have been found to interact with Rho GEFs (18). These interactions result in targeting of the Rho GEFs to specific locations within the cell, in the restriction of the nucleotide exchange activity of Rho GEFs and also affect the spatial and temporal activation of the downstream GTPases (5, 11, 12, 37, 46, 47, 50).

Neuroepithelioma transforming gene 1 (Net1) is a RhoA-specific GEF that was originally identified in a genetic screen

* Corresponding author. Mailing address: Department of Cell and Developmental Biology, University of North Carolina at Chapel Hill, 12-026 Lineberger, CB#7295, Chapel Hill, NC 27599. Phone: (919) 966-5783. Fax: (919) 966-3015. E-mail: rafaelgm@med.unc.edu.

† Supplemental material for this article may be found at http://mcb.asm.org/.

▽ Published ahead of print on 15 October 2007.

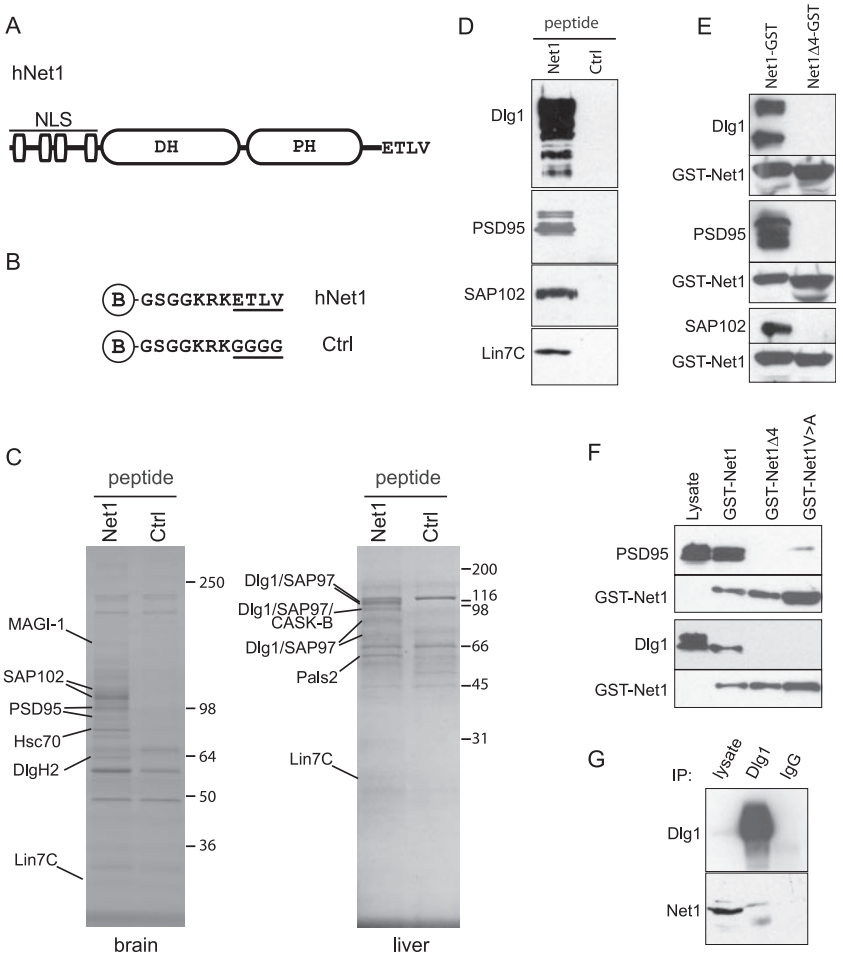

FIG. 1. Mouse brain, kidney, or liver lysates were incubated with streptavidin-Sepharose beads coupled with biotinylated peptides corresponding to the last 10 amino acids of Net1 or control (ctrl) peptides in which the last 4 amino acids were replaced by glycine (underlined). After being washed, the samples were separated by SDS-PAGE and the indicated bands were identified by MS as described in Materials and Methods. (A) Domain structure of the Net1 protein. (B) Peptide sequences used in this study. The peptides were biotinylated and contained an N-terminal glycine residue as a spacer. (C) SDS-PAGE gels from two representative experiments showing the proteins identified. Gels were stained with Coomassie blue. The bands of interest were cut from the gel and identified at the MS facility at UNC. Molecular mass markers (kDa) are indicated in each panel. (D) Protein identities were confirmed by Western blot analysis using commercially available antibodies. Peptide pulldowns were performed as described for panel C. Proteins were separated by SDS-PAGE and immunoblotted for PSD95, Dlg1, SAP102, and Lin7C. (E) Pulldown assay using brain lysates (PSD95, SAP102, and Lin7) or liver lysates (Dlg1) and GST-Net1 or a deletion mutant missing the PDZ-binding motif (GST-Net1Δ4). The precipitated proteins were immunoblotted with anti-PSD95, anti-Dlg1, and anti-SAP102 antibodies. The same blot was subsequently stripped and immunoblotted using anti-Net1 antibodies to verify the levels of GST-Net1 constructs in the assay. (F) Pulldown assay using brain lysates (PSD95) or liver lysates (Dlg1) and GST-Net1; a deletion mutant missing the PDZ-binding motif (GST-Net1Δ4) or a single-amino-acid-substitution mutant in the PDZ-binding motif (GST-Net1V→A). The precipitated proteins were immunoblotted with anti-PSD95 and anti-Dlg1 antibodies. The same blot was subsequently stripped and immunoblotted using anti-Net1 antibodies to verify the levels of GST-Net1 constructs in the assay. (G) Coprecipitation of endogenous Dlg1 and Net1 from HEK293 lysates. HEK293 lysates were incubated with anti-Dlg1 or with control antibodies, and the precipitates (IP) were immunoblotted for Net1. Net1 coprecipitated only with Dlg1, not with control antibodies.

for novel oncogenes (8). The NET1 gene encodes a 595-amino-acid protein that consists of an N-terminal domain containing a series of nuclear localization signals (NLS), a DH-PH domain, and a short C-terminal domain carrying a consensus PDZ-binding motif (Fig. 1A). At steady state, Net1 localizes to the nucleus through the function of its NLS (55). Deletion of the N-terminal domain containing the NLS sequences redistributes Net1 to the cytosol and promotes the formation of actin stress fibers, which is a consequence of RhoA activation (2, 55). The oncogenic Net1 clone isolated in the original screen encoded a truncated protein in which the first 145 amino acids, including the NLS, were missing, suggesting that relocalization of the RhoA exchange activity to the cytosol was responsible for the transformation ability of Net1 (8, 55). However, further studies demonstrated that a high exchange activity in the cytosol was not sufficient to induce transformation (49). In addition, these studies demonstrated that the PDZ-binding motif was essential for Net1-mediated transformation of NIH 3T3 cells, suggesting that the interaction between Net1 and a PDZ domain protein could be playing a role.

In this study, we show that PDZ domain-containing proteins of the membrane-associated guanylate kinase (MAGUK) fam-

ily, including the tumor suppressor Dlg1/SAP97, bind to Net1. Their interaction results in the translocation of its PDZ partners to subnuclear structures associated with promyelocytic leukemia protein (PML) bodies. In contrast, the oncogenic mutant of Net1 which lacks the NLS binds to and sequesters these same PDZ proteins in the cytosol. Our results suggest that the interaction between Net1 and tumor suppressor proteins such as Dlg1 or SAP102 may contribute to the mechanism of Net1-mediated transformation.

MATERIALS AND METHODS

Antibodies and cDNA constructs. The following antibodies were used: anti-PSD95 (Upstate); anti-SAP97/Dlg1 (StressGen); anti-Dlg1, anti-RhoA, and anti-phosphotyrosine (PY99) (Santa Cruz); antiphosphothreonine and antiphosphoserine (Zymed); anti-SAP102, polyclonal anti-myc, and anti-Net1 (AbCam); anti-Lin7, antitubulin, antivinculin, and anti-FLAG (M2) (Sigma); anti-LaminA/C (BD Biosciences); antiactin (clone 1501) (Calbiochem); monoclonal anti-myc (Invitrogen); and anti-green fluorescent protein (anti-GFP) (Roche). Antibodies against SC35, PML, and coilin were a kind gift from Karl Fu (University of Alabama at Birmingham). For Western blotting, the primary antibodies were detected using horseradish peroxidase-conjugated secondary antibodies (Jackson Inmmunoresearch) with SuperSignal West Pico detection reagents (Pierce). Alexa 594-, 488-, and 350-conjugated anti-mouse and anti-rabbit secondary antibodies were from Molecular Probes. Alexa 594-phalloidin was from Molecular Probes. Rat PSD95 fused to GFP and rat SAP102 in pCDNA3 were generous gifts from Mike Ehlers (Duke University). SAP102 was subcloned into pEGFP-C2 (Clontech). Mouse Dlg1 was purchased from Open Biosystems (no. 9200268) and subcloned into pEGFP-C2. Net1 and Net1A cDNAs were purchased from Origene and subcloned into pCMVmyc (Clontech). mCherry was a kind gift from Klaus Hahn (University of North Carolina [UNC]). Deletion mutants were made using conventional PCR cloning techniques. Δ4 mutations (NetΔ4 and NetΔNΔ4) were made by introducing a stop codon before the PDZ-binding motif, using a QuikChange II mutagenesis kit (Stratagene). V→A and L267E substitutions were also made using a QuikChange II mutagenesis kit. All constructs were verified by DNA sequencing.

Cell culture and transfection. HeLa cells were cultured in modified Eagle's medium (Invitrogen) supplemented with nonessential amino acids, 10% fetal bovine serum (FBS) (Sigma), and antibiotics (penicillin-streptomycin). HEK293 cells were cultured in Dulbecco's modified Eagle's medium (DMEM) (Invitrogen) supplemented with nonessential amino acids, 10% FBS, and antibiotics. NIH 3T3 cells were cultured in DMEM supplemented with 10% bovine calf serum and antibiotics (Sigma). MCF10a cells were cultured in DMEM-F12 (Invitrogen) supplemented with 5% horse serum (Invitrogen), 20 ng/ml epidermal growth factor (Sigma), 0.01 mg/ml insulin (Invitrogen), 500 ng/ml hydrocortisone (Invitrogen), and antibiotics. MCF7 cells were grown in minimal essential medium (Invitrogen) supplemented with FBS, Na pyruvate (Invitrogen), and antibiotics. Cells were transfected using FuGene6 or FuGene HD (Roche) according to the manufacturer's instructions.

Small interfering RNA (siRNA) against human Net1 was from Dharmacon Research. The RNA sequences were as follows: sense, 5′-GAGUCUCCCUUC AGUCGAAUU-3′, and antisense, 5′-UUCGACUGAAGGGAGACUCUU-3′. As a control, we used si*GLO* RISC-Free nontargeting siRNA (Dharmacon). HEK293 cells were transfected using the TransIT siQuest transfection reagent (Mirus), following the manufacturer's instructions. Cells were assayed 96 h after transfection.

Peptide pulldowns. Tissues were homogenized in a Dounce homogenizer in 5 volumes of buffer HNMD (HEPES-KOH, 50 mM [pH 7.4]; NaCl, 150 mM; $MgCl_2$, 1 mM; dithiothreitol [DTT], 1 mM; and freshly added protease inhibitors and 1% Triton X-100). The homogenates were then centrifuged for 15 min at 27,000 × *g*. The supernatants (10 mg/experiment at 1 mg/ml) were then precleared for 1 h at 4°C using streptavidin-Sepharose beads (100 μl) (GE). At the same time, 40 μg of peptide was incubated with 40 μl of streptavidin beads in HNMD for 1 h at 4°C. The beads were then washed three times with HNMD and incubated with 10 mg of precleared lysate for 1 h at 4°C on a rotating platform. The beads were then washed three times in binding buffer, resuspended in 30 μl of sodium dodecyl sulfate (SDS) sample buffer, boiled for 10 min, and separated by SDS-polyacrylamide gel electrophoresis (PAGE). The bands of interest were then identified by matrix-assisted laser desorption ionization–time of flight mass spectrometry (MS), and selected tryptic peptides were sequenced by Nano-ESI tandem MS at the UNC proteomics facility.

GST pulldowns and immunoprecipitation. Cells were washed twice in phosphate-buffered saline (PBS), lysed in lysis buffer (HEPES-KOH, 50 mM [pH 7.4]; NaCl, 150 mM; $MgCl_2$, 1 mM; DTT, 1 mM; and freshly added protease inhibitors and 1% Triton X-100) and centrifuged at 16,000 × *g* for 15 min at 4°C. Tissue lysates were prepared as described above. Glutathione *S*-transferase (GST)-tagged proteins bound to glutathione-Sepharose (GE) were incubated with lysates for 1 h at 4°C. The beads were then washed three times in lysis buffer, resuspended in 30 μl of SDS sample buffer, boiled for 10 min, and separated by SDS-PAGE. Proteins were then transferred to nitrocellulose and immunoblotted with the indicated antibodies. For immunoprecipitation, cell lysates were incubated with antibodies (2 μg) and incubated for 1 h at 4°C. Protein G-Sepharose (GE) was then added and incubated for 45 min at 4°C. Immune complexes were recovered by centrifugation, washed three times with lysis buffer, and boiled in SDS sample buffer. After SDS-PAGE, proteins were transferred to nitrocellulose and immunoblotted with the indicated antibodies.

RhoA activity pulldowns. Construction of the pGEX4T-1 prokaryotic expression constructs containing the Rho binding domain (RBD) of rhotekin have been described previously (36). Briefly, expression of the fusion proteins in *Escherichia coli* was induced with 100 μM IPTG (isopropyl-β-D-thiogalactopyranoside) for 12 to 16 h at room temperature. Bacterial cells were lysed in buffer containing 50 mM Tris (pH 7.6), 150 mM NaCl, 5 mM $MgCl_2$, 1 mM DTT, 10 μg/ml each of aprotinin and leupeptin, and 1 mM phenylmethylsulfonyl fluoride (PMSF) and the proteins purified by incubation with glutathione-Sepharose 4B beads (GE) at 4°C. Active RhoA pulldown experiments were performed as described elsewhere (3). Briefly, suspended and adherent cells were lysed in 50 mM Tris (pH 7.6), 500 mM NaCl, 1% Triton X-100, 0.1% SDS, 0.5% deoxycholate, 10 mM $MgCl_2$, 200 μM orthovanadate, and protease inhibitors. Lysates were clarified by centrifugation, equalized for total volume and protein concentration, and rotated for 30 min with 30 μg of purified GST-RBD bound to glutathione-Sepharose beads. The bead pellets were washed in 50 mM Tris (pH 7.6), 150 mM NaCl, 1% Triton X-100, 10 mM $MgCl_2$, 200 μM orthovanadate, and protease inhibitors and subsequently processed for SDS-PAGE.

Subcellular fractionation. Intact nuclei were isolated using an iodixanol (OptiPrep; Axis Shield) discontinuous gradient according to the manufacturer's instructions. Briefly, cells were rinsed three times with PBS and scraped in homogenization medium (0.25 M sucrose, 25 mM KCl, 5 mM $MgCl_2$, 20 mM Tris-HCl, pH 7.8, 10 μg/ml each of aprotinin and leupeptin, and 1 mM PMSF). Cells were then centrifuged for 10 min at 1,000 × *g*, and the pellet was resuspended in homogenization medium. The cell suspension was homogenized using 20 strokes of the pestle of a tight-fitting Dounce homogenizer. Homogenization was monitored under a phase-contrast microscope until >90% of the cells were broken. The homogenate was then centrifuged to produce a crude nuclear pellet (1,000 × *g* for 10 min) and resuspended in homogenization medium. Equal volumes of the crude nuclear pellet and a 50% iodixanol solution were then mixed and layered on top of a 30% to 35% discontinuous iodixanol gradient. The samples were then centrifuged at 10,000 × *g* for 20 min in a swinging bucket rotor. The nuclear fraction (30 to 35% interface) was collected, diluted with 2 volumes of homogenization medium, and centrifuged for 10 min at 1,000 × *g*. The pellet fraction, which contains nuclei, was resuspended in 100 μl of ice-cold nuclear extraction buffer (20 mM HEPES, pH 7.9, with 1.5 mM $MgCl_2$, 0.42 M NaCl, 0.2 mM EDTA, 25% [vol/vol] glycerol, 10 μg/ml each of aprotinin and leupeptin, and 1 mM PMSF) and vortexed at the highest setting for 15 seconds every 10 min for a total of 40 min of extraction. The samples were then briefly sonicated and centrifuged at maximum speed (~16,000 × *g*) in a microcentrifuge for 10 min, and the supernatant (nuclear extract) fraction was transferred to a clean, prechilled tube. Samples were stored at −80°C until use.

Immunofluorescence microscopy. Cells grown on coverslips were washed in PBS, fixed in 3.7% paraformaldehyde for 10 min, and quenched with 10 mM ammonium chloride in PBS. Cells were permeabilized with 0.1% Triton X-100 in PBS for 10 min. The coverslips were then washed with PBS and blocked in PBS plus 2.5% goat serum and 0.2% Tween 20 for 5 min, followed by blocking in PBS plus 0.4% fish skin gelatin and 0.2% Tween 20. Cells were incubated with primary antibody for 1 h at room temperature. Coverslips were washed five times for 5 min with PBS plus 0.2% Tween 20 and incubated with secondary antibodies for 45 min. Coverslips were washed as described above and mounted on slides in 9:1 glycerol-PBS with 0.1% *p*-phenylenediamine. Epifluorescence images were captured with a Zeiss Axiovert 200 M microscope equipped with a Hamamatsu ORCA-ERAG digital camera and Metamorph Workstation (Universal Imaging Corp.). Quantitative analysis was performed using Metamorph to measure the average fluorescence intensity per cell in images that were serially acquired using the same illumination and exposure parameters. Confocal image acquisition and analysis were performed using a Leica SP2 AOBS confocal microscope with a 63×, 1.4-numerical-aperture apochromatic Leica lens (Leica Microsystems).

Scanning was performed with the *xy* axis, using three independent laser sources (364-nm-UV, 488-nm-Ar, 568-nm-Kr lasers), as required. Images were processed using Leica and Adobe Photoshop software.

Focus formation assays. Primary focus formation assays were performed with NIH 3T3 cells as described previously (58). Briefly, NIH 3T3 cells were transfected using the Amaxa nucleofection system (6 to 8 μg of DNA/1 × 10^6 to 2 × 10^6 cells) and plated into three 6-cm-diameter dishes. Twenty-four hours after transfection, the bovine calf serum concentration was reduced from 10% to 5%. Medium was changed every 2.5 days. Cells were fixed 12 to 14 days later and stained with a solution containing 30% methanol and 0.4% crystal violet. Foci larger than 1 mm in diameter were scored.

Electron microscopy. HeLa cells were plated on coverslips and grown for 24 h. Cells were then transfected and chemically fixed in 2.5% glutaraldehyde and 1% tannic acid in 0.1 M cacodylate buffer (pH 7.3) for 1 h at 4°C. Following fixation, cells were washed with 0.1 M cacodylate buffer, treated for 1 h with cold 0.5% osmium tetroxide, washed with water and once with 50% ethanol, stained with 2% uranyl acetate in the dark for 30 min, and dehydrated through a graded ethanol series. Sections were infiltrated and embedded in an epoxy resin (EMbed-812; Electron Microscopy Sciences). Vibratome sections were bisected along the equatorial and optic axes and mounted for ultramicrotome sectioning. Mesas were raised in the regions of interest, and 55-nm thin sections were cut with a diamond knife (Diatome). The sections were collected on copper grids and stained with uranyl acetate and lead citrate. The specimens were examined using an FEI Philips Tecnai 12 TEM electron microscope (FEI Company) at 80 kV. Images were captured using a Gatan 794 digital camera (Gatan Inc.) and Digital Micrograph software (Gatan Inc.).

RESULTS

Interaction between Net1 and PDZ-containing proteins. We used a peptide pulldown approach coupled with MS analysis to determine if the PDZ-binding motif present at the C terminus of Net1 was able to bind PDZ domain-containing proteins. We synthesized an NH_3-biotinylated peptide corresponding to the last 10 amino acids of human Net1 as well as a control peptide in which the last 4 amino acids were replaced by glycine (Fig. 1B). We then used these peptides to isolate binding proteins from different mouse tissues, including brain, liver, and kidney. The proteins were separated in an SDS-PAGE gel and stained with Coomassie blue dye. The bands of interest were cut from the gel and identified by MS. Shown in Fig. 1C are the results of two representative pulldowns from brain and liver. Although there were some bands that appeared in both the peptide and the control lane, several other bands were found exclusively in the peptide lane. As shown in Fig. 1C, we were able to identify most of the peptide-specific bands by MS. Almost all of the proteins identified, with the exception of Hsc70, correspond to PDZ domain-containing proteins, including PSD95/SAP90/Dlg4, SAP102/Dlg3, MAGI-1, and Dlgh2/MAGUK-p55 in brain; Dlg1/SAP97, Pals2, and mCASK-B in liver; and Veli3/Lin7C in both brain and liver as well as in kidney. The identities of a selected set of the interacting proteins were confirmed by Western blot analysis using commercially available antibodies. Figure 1D shows that when peptide pulldowns similar to the ones used for MS analysis were transferred to nitrocellulose and immunoblotted with Dlg1, SAP102, PSD95, and Lin7C antibodies, the expected proteins were exclusively detected in the Net1 peptide lane but not in the control lane. In addition, we used full-length Net1 fused to GST to determine whether the full-length protein also coprecipitated with the same proteins that we observed in the peptide pulldowns. As a control, we used a similar GST fusion protein, in which the last four amino acids, carrying the PDZ-binding motif, had been deleted (Net1Δ4-GST) or a single-amino-acid-substitution mutant in which the C-terminal amino acid valine was replaced by an alanine (Net1V→A-GST). In agreement with the results from the peptide pulldowns, only the full-length Net1 protein was able to interact with PSD95, Dlg1, and SAP102, not the Δ4 mutant or the V→A mutant, suggesting that these interactions were specifically mediated by the PDZ-binding motif at the C terminus of Net1 (Fig. 1E and F). This interaction is direct and requires PDZ domains 1 and 2 from Dlg1 (H. S. Carr and J. A. Frost, personal communication). To confirm that the interaction also occurred with endogenous proteins, we immunoprecipitated Dlg1 from HEK293 lysates and blotted for Net1. As shown in Fig. 1G, Net1 coimmunoprecipitated with Dlg1 antibodies but not with control antibodies. In addition, we were able to coimmunoprecipitate endogenous Dlg1 and Net1 from purified nuclei (see Fig. S3B in the supplemental material). The reverse coimmunoprecipitation could not be performed successfully, because the Net1 antibodies available were raised against a peptide corresponding to the Net1 C terminus, which includes the PDZ-binding tail, a region that is probably masked when the two proteins interact.

Interaction with Net1 causes the relocalization of Dlg proteins from the cytosol to defined nuclear subdomains. In many cases, the interaction of a protein with a PDZ domain-containing protein plays a role in targeting the protein to a specific cellular localization. In particular, PDZ scaffolding proteins such as PSD95, Dlg1, and SAP102 have been shown to concentrate or cluster neurotransmitter receptors at the plasma membrane in the postsynaptic dendritic spines (13, 27, 56). This same effect was observed when the two interaction partners were transfected in a heterologous cell system (31, 32). Since Net1 shuttles between the nucleus and the cytosol, we hypothesized that its interaction with a PDZ protein in the cytosol may play a role in targeting and/or sequestering Net1 in the cytosol, where it can activate RhoA and perform its cellular function. To test this hypothesis, we cotransfected full-length, myc epitope-tagged Net1 with PSD95, SAP102, or Dlg1 into HeLa cells. Each PDZ protein was fused to GFP to allow for visualization of its localization. Our results show that, as previously reported, Net1 localized to the nucleus and to some extent to the cytosol when singly transfected (Fig. 2A) (1, 49, 55).

Interestingly, cotransfection of Net1 with PSD95, Dlg1, or SAP102 induced a striking redistribution of these PDZ proteins from a diffuse cytosolic staining (Fig. 2C) to a series of spatially restricted subdomains inside the nucleus (Fig. 2B). In any given experiment, approximately 60% of the cotransfected cells presented these nuclear clusters. The nuclear structures differed in shape, size, and number, ranging from 2 to 83 clusters per cell (average = 26.4 clusters/cell), with a typical size ranging between 0.1 and 1 μm^2. With epifluorescence, the signal for Net1 in the nucleus was too bright to determine if Net1 colocalized with the PDZ proteins in these nuclear clusters. However, analysis using confocal microscopy showed a high degree of colocalization between Net1 and its interaction partners (Fig. 2D). Identical results were observed in COS-7, HEK293, and NIH-3T3 cells, indicating that this was a general effect and not a cell line-specific result (data not shown). At the ultrastructural level, cotransfected cells contained a collection of electron-dense particles distributed throughout the nucleus, ranging from 0.1 μm to 2 μm in diameter, that were not

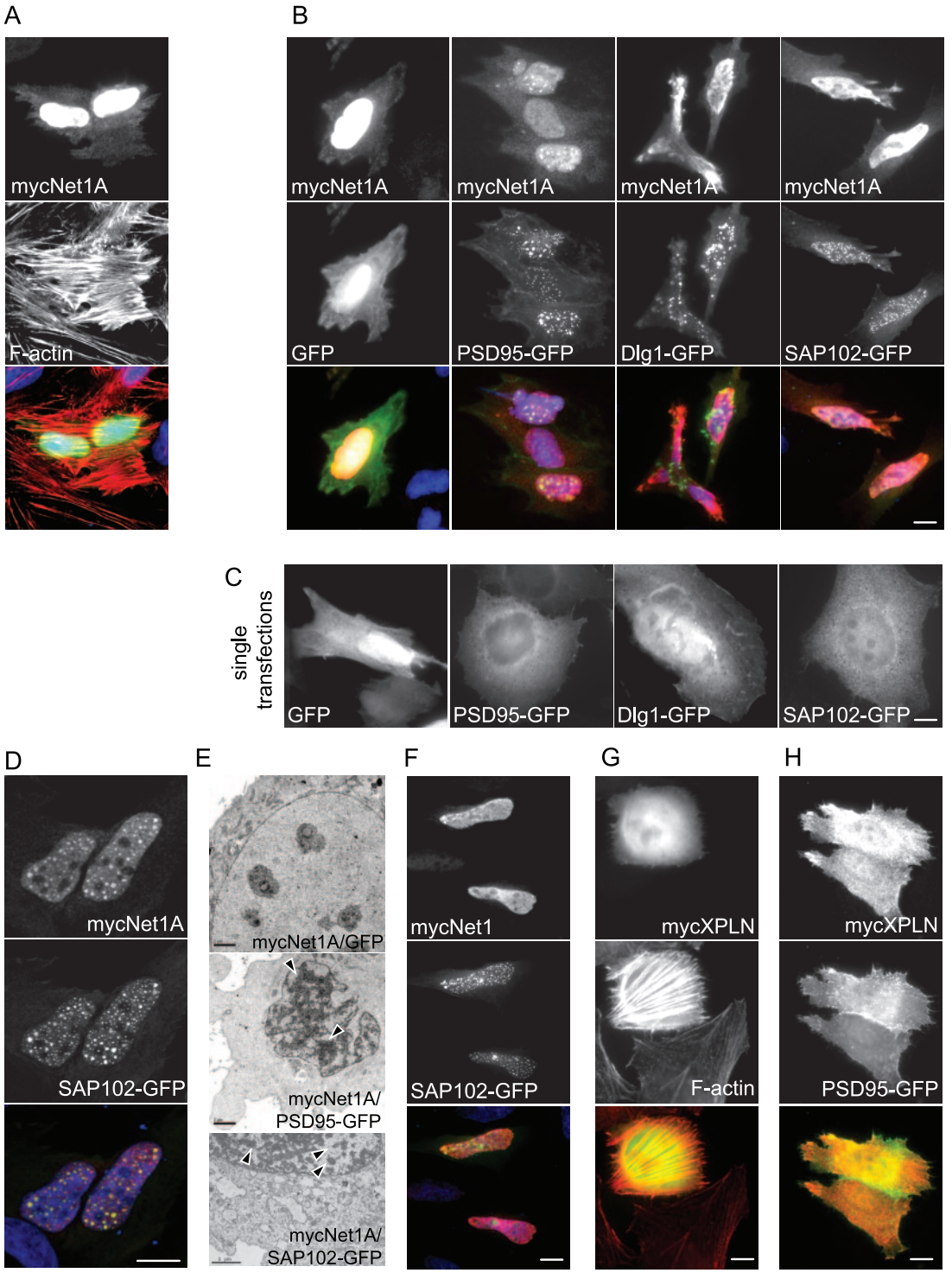

FIG. 2. HeLa cells were cotransfected with myc-Net1A and either PSD95-GFP, Dlg1-GFP, SAP102-GFP, or GFP alone; processed for immunofluorescence using anti-myc antibodies (red); and analyzed also for the GFP signal (green). Actin was stained with Alexa 594-phalloidin. Nuclear DNA was stained with Hoechst (blue). (A) Net1A localizes to the nucleus and to some extent to the cytosol when transfected alone. (B) Cotransfection of Net1A with any of the Dlg proteins induces a striking redistribution from a diffuse cytosolic staining (C) to a series of restricted subdomains within the nucleus. (C) The three Dlg proteins show a diffuse distribution in the cytosol in singly transfected cells. (D) Confocal sections show that both Net1 and SAP102 colocalize within the nuclear subdomains. (E) Ultrastructural analysis shows electron-dense particles in cells cotransfected with Net1A and PSD95-GFP or SAP102-GFP (arrowheads) that are not present in control cells and also severely distorted nuclei. (F) Identical subnuclear structures were formed when Net1 was cotransfected with SAP102. (G, H) The formation of the nuclear subdomains was not induced by coexpression of PSD95-GFP and XPLN, a protein homologous to Net1. Bar = 10 μm in all panels except panel E (bar = 2 μm).

present in control cells cotransfected with Net1 and an empty GFP vector (Fig. 2E). Our initial experiments were carried out using a splice variant of Net1, Net1A. However, identical results were observed with the longer isoform, Net1, in all the experiments that we performed (Fig. 2F and 3E for quantification; also data not shown). In the text, Net1 is used to reference either Net1 or Net1A. However, each figure indicates which particular isoform was used in each experiment. In order to determine if this effect was specific to Net1, we performed similar experiments using a related Rho GEF, XPLN/ARHGEF3. XPLN is the closest Net1 homologue in the human genome (54% identity, 66% homology). It is RhoA specific and induces the formation of actin stress fibers upon overexpression (4) (Fig. 2G). XPLN also contains a PDZ-binding motif at the C terminus and is able to coprecipitate with PSD95 in peptide pulldowns (data not shown). However, when PSD95 was coexpressed with XPLN, it did not redistribute to the nucleus, suggesting that the nuclear localization of PSD95 was specific for Net1 (Fig. 2H and 3E for quantification).

Deletion of the PDZ-binding motif in Net1 prevents the relocalization of the PDZ proteins and the formation of nuclear clusters. To determine whether the effects that we observed were specifically caused by the interaction between the PDZ-binding motif of Net1 and the PDZ domain of each protein, we eliminated the PDZ-binding site within Net1A by introducing a stop codon (Net1Δ4). We have shown in Fig. 1 that the equivalent mutation in a NET-GST fusion protein blocked binding to PSD95, Dlg1, and SAP102 in pulldown experiments. We observed that the Net1Δ4 mutant behaved like the full-length Net1 protein when transfected alone, localizing predominantly to the nucleus and causing the formation of actin stress fibers when expressed at high levels (Fig. 3A). Importantly, when Net1Δ4 was coexpressed with PSD95, Dlg1, or SAP102, the relocalization of the PDZ proteins to the nucleus and the formation of nuclear clusters were completely abolished (Fig. 3B and E for quantification). Instead, each of these proteins showed a diffuse, cytosolic pattern that was indistinguishable from that observed when they were expressed alone (Fig. 2B). These results demonstrate that Net1 must interact with PDZ domain proteins through its PDZ-binding site to cause their nuclear relocalization.

Formation of the nuclear clusters is independent of the exchange activity of Net1. We next wanted to examine the role of Net1 nucleotide exchange activity in the relocalization of the PDZ proteins and the formation of the nuclear clusters. To address this, we generated a single-amino-acid-substitution mutant which has been previously shown to inhibit the catalytic activity of Net1 (L321E in Net1, L267E in Net1A) (2). As expected, overexpression of the inactive Net1 protein in HeLa cells had no effect on stress fiber formation (Fig. 3C). Interestingly, cotransfection of Net1-L267E with PSD95, Dlg1, or SAP102 did not prevent the formation of nuclear clusters (Fig. 3D and F). Similarly, a mutation in the PH domain (Net1W492L) previously described as catalytically inactive (2) was as efficient as wild-type Net1 in its ability to recruit Dlg proteins to the nucleus and target them to nuclear clusters (data not shown). Taken together, these results demonstrate that the relocalization of PDZ proteins into the nucleus and the formation of nuclear clusters do not require Net1-mediated RhoA activation.

The interaction between Net1 and Dlg proteins has no effect in Net1-mediated RhoA activation. As shown in Fig. 3, the formation of the nuclear clusters was not inhibited by abrogating the exchange activity in Net1. However, that did not eliminate the possibility that the interaction between Dlg proteins and Net1 had an effect on Net1 exchange activity on RhoA. To determine if this was the case, we transfected HeLa cells with Net1ΔN alone or in combination with two members of the Dlg family, Dlg1 and SAP102. We then analyzed their effect on RhoA activity by looking at the formation of stress fibers in transfected cells. As shown in Fig. 4, overexpression of Net1ΔN induces a striking increase in the formation of stress fibers. In contrast, neither Dlg1 nor SAP102 by itself had any effect on stress fiber formation. When Dlg1 or SAP102 was cotransfected with Net1ΔN, we could not detect any significant difference from cells singly transfected with Net1ΔN, suggesting that the interaction was not affecting Net1 exchange activity. Quantitation of F-actin fluorescence intensity supports our conclusion and shows that there is no significant difference between cells transfected with Net1ΔN and those cotransfected with Dlg protein (Fig. 4C). We also measured RhoA GTP levels in a similar set of transfected cells by using a pulldown assay. The results of the pulldown assay show essentially the same results as those observed in the immunofluorescence analysis, that is, Net1ΔN induces RhoA activation compared to what occurs in nontransfected, starved cells. This activity is not affected significantly by cotransfecting Dlg1 or SAP102 (Fig. 4D). Taken together, our results suggest that the interaction between Net1 and Dlg proteins does not seem to be involved in the regulation of Net1's exchange activity.

Characterization of the nuclear clusters. There were a number of possible explanations for the formation of the nuclear clusters that we observed. For example, a number of different nuclear subdomains that resemble the Net1-PDZ protein clusters have been characterized, including PML bodies, nuclear speckles, and Cajal bodies (26, 59). However, it was also possible that the nuclear clusters were artifactual. For example, proteins that tend to form aggregates such as polyglutamine repeat-containing proteins have been shown to form nuclear aggregates of similar size and shape (9, 57, 61, 72). Similarly, overexpression of GFP chimeras has also been associated with misfolding and aggregation (15, 17, 35). To rule out the possibility that the addition of GFP to the PDZ domain proteins resulted in the nuclear clusters that we observed, we replaced the GFP tag in some of the proteins with a smaller FLAG tag and coexpressed it with Net1. As shown in Fig. 5A, the FLAG-tagged Dlg1 and SAP102 proteins, upon coexpression with Net1, translocated to nuclear subdomains that were indistinguishable from those formed by the GFP-tagged constructs. To determine whether the Net1-induced nuclear clusters corresponded to identifiable nuclear structures, we stained cells cotransfected with Net1 and PSD95, Dlg1, or SAP102 with known markers for nuclear subdomains. These markers included PML protein for PML bodies, SC35 for nuclear speckles, and coilin for Cajal bodies. Figure 5B shows that of all markers tested, only PML bodies colocalized with the clusters induced by Net1 (shown for SAP102). In general, PML bodies were located adjacent to or showed partial colocalization with

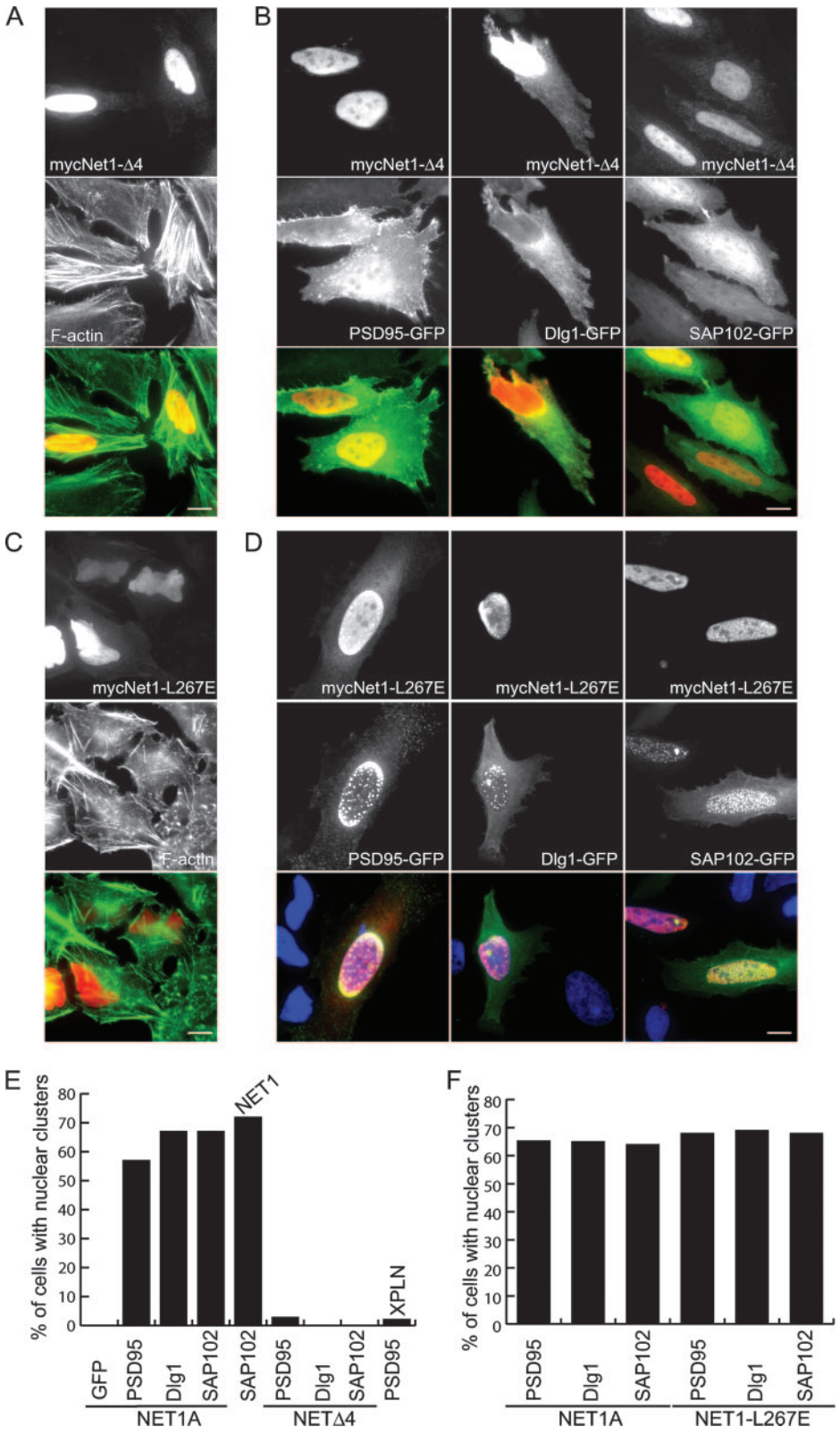

FIG. 3. HeLa cells were cotransfected with a Net1A mutant in which the last four amino acids, corresponding to the PDZ-binding motif, have been deleted (Net1Δ4) and either PSD95-GFP, Dlg1-GFP, SAP102-GFP, or GFP as a control and processed for immunofluorescence using anti-myc antibodies (red). Cells were also analyzed for the GFP signal (green). (A) Net1Δ4 localizes to the nucleus and induces actin stress fibers in a manner indistinguishable from that of wild-type Net1. (B) When Net1Δ4 is coexpressed with PSD95, Dlg1, or SAP102, the relocalization of these proteins to the nucleus and the formation of nuclear clusters are completely abolished. The three Dlg proteins also show a diffuse localization that is identical to that observed when they are expressed alone. (C) Catalytically inactive Net1 (L267E) fails to induce stress fibers when overexpressed in HeLa cells. (D) When the catalytically inactive Net1 protein is cotransfected with either PSD95, Dlg1, or SAP102, the formation of nuclear subdomains is not affected, suggesting that it is not dependent on the nucleotide exchange activity of Net1. (E, F) Experiments for Fig. 2B, 2H, 3B and 3D were quantified. At least 200 cells were counted for each condition and scored for the presence or absence of nuclear subdomains. Bar = 10 μm in all panels.

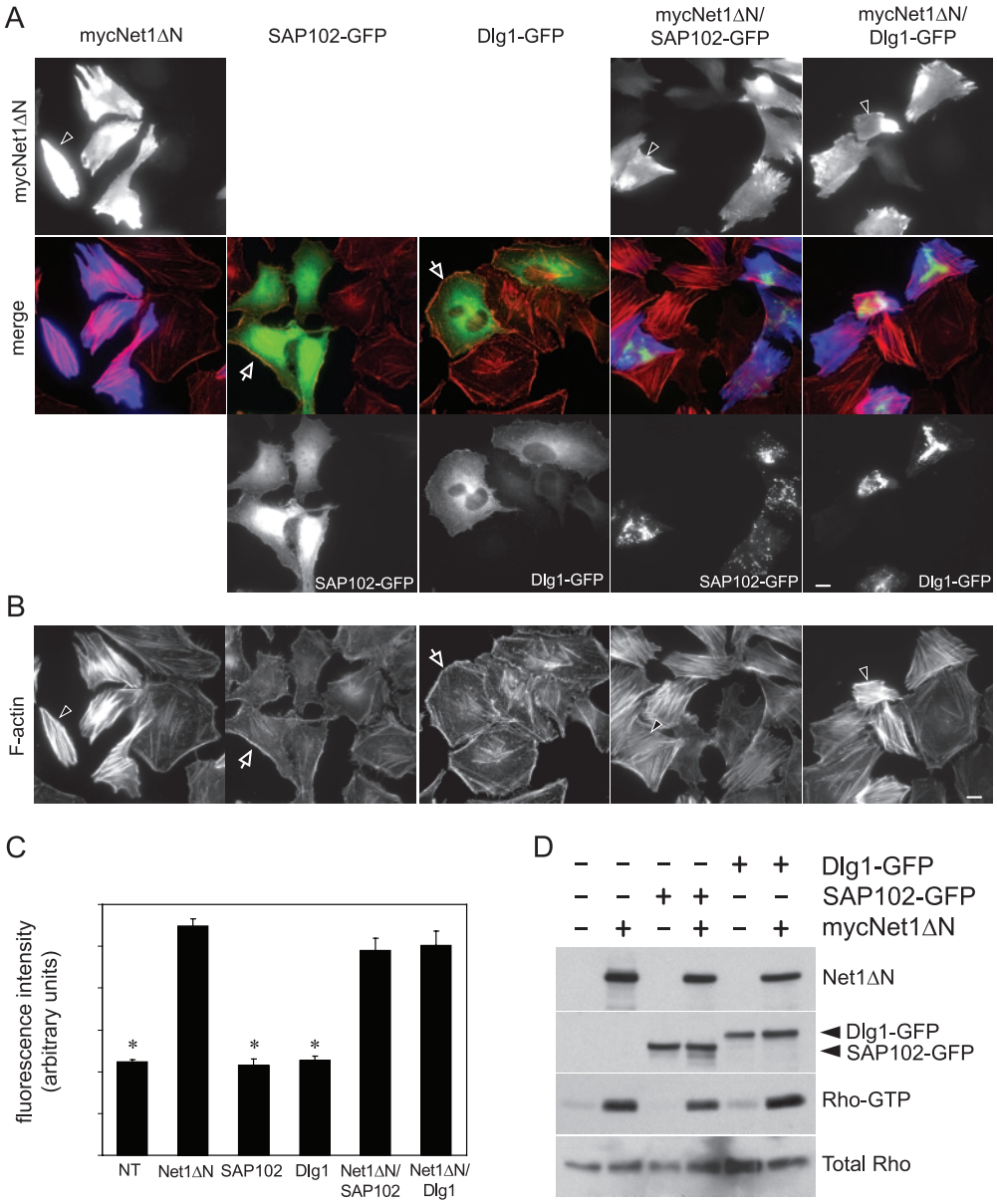

FIG. 4. HeLa cells were transfected with mycNet1ΔN, Dlg1-GFP, or SAP102-GFP alone or in combination as indicated in the figure and processed for immunofluorescence by using monoclonal anti-myc antibodies (blue) and Alexa 594-phalloidin (red). Cells were also analyzed for the GFP signal (green). (A, B) Overexpression of Net1ΔN (the arrowhead indicates a representative cell) but not Dlg1-GFP or SAP102-GFP (arrow) induces the formation of stress fibers. Coexpression of Dlg1-GFP or SAP102-GFP with Net1ΔN does not affect Net1-mediated stress fiber formation (the arrowhead indicates a representative cell transfected with either Dlg1-GFP or SAP102-GFP with Net1ΔN). (A) A representative panel for each transfection is shown. The constructs used for each condition are indicated on top of each panel. (B) Alexa 594-phalloidin-stained images used for quantification. A representative image is shown. Arrowheads indicate cells transfected with the constructs indicated in panel A. (C) To quantify stress fiber formation, the average fluorescence intensity per cell in the red channel was measured. The fluorescence intensities in the green and blue channels were also measured to identify transfected cells. All images were acquired using the same exposure parameters. At least 25 cells were counted for each condition. Significance of difference from the control (Net1ΔN) was estimated by Student's *t* test for nonpaired values. Bars not significantly different from the control values were left unmarked. An asterisk signifies a *P* value of <0.001. Bar = 10 μm in all panels. (D) HEK293 cells were transfected with mycNet1ΔN, Dlg1-GFP, or SAP102-GFP alone or in combination as indicated in the figure. Active Rho was specifically pulled down from cell lysates containing equal amounts of proteins with immobilized recombinant RBD-GST and analyzed by Western blotting using anti-RhoA antibody. Results for a representative experiment are shown.

the structures containing Net1 and PDZ proteins. We observed a better colocalization with PML bodies in nuclear clusters that were bigger, suggesting that smaller clusters may coalesce and form bigger structures that could eventually associate with the PML bodies, as has been shown for other proteins (15, 44). In contrast, SC35, the marker for nuclear speckles, showed a pattern that was mutually exclusive with that of the GFP-Dlg clusters, suggesting that the Net1-induced nuclear domains were not speckles (Fig. 5B). Cajal bodies colocalized to some extent with the GFP-Dlg clusters (Fig. 5B).

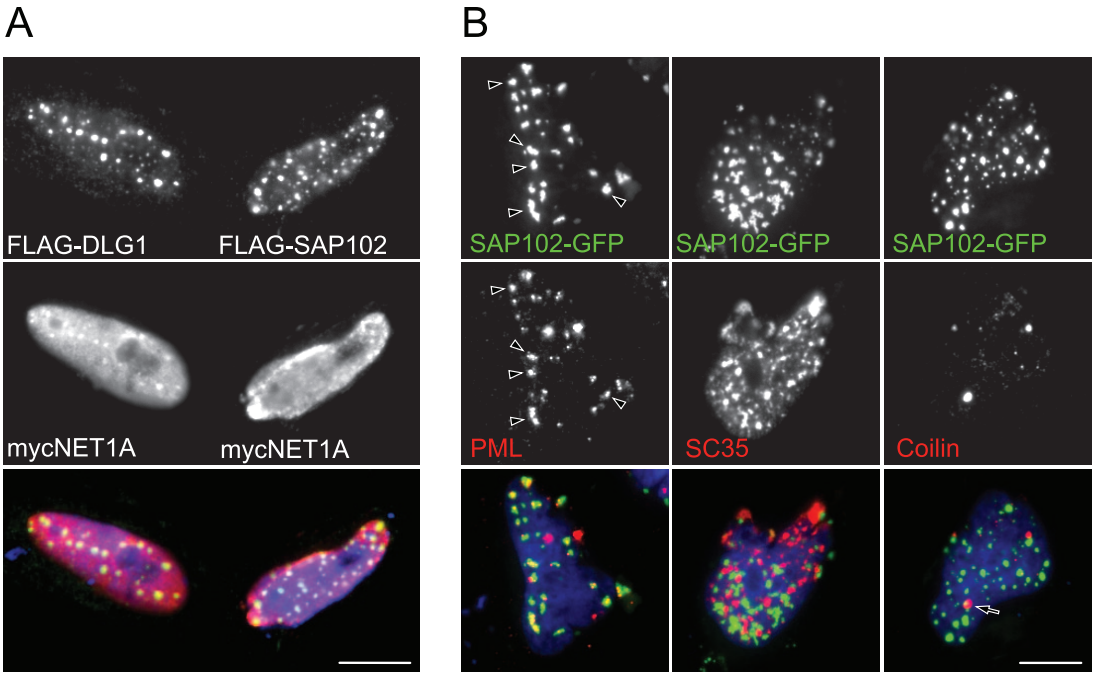

FIG. 5. (A) HeLa cells were cotransfected with myc-Net1A and either FLAG-Dlg1 or FLAG-SAP102 and processed for immunofluorescence using anti-FLAG (green) and anti-myc (red) antibodies. FLAG-tagged Dlg1 and SAP102 form nuclear subdomains that are identical to those formed by the GFP-tagged proteins, suggesting that GFP is not promoting the formation of these structures. (B) HeLa cells were cotransfected with myc-Net1A and either PSD95-GFP, Dlg1-GFP, or SAP102-GFP and processed for immunofluorescence using anti-PML (PML bodies), anti-SC35 (speckles), and anticoilin (Cajal bodies) antibodies (red) and analyzed also for the GFP signal (green). PML bodies showed partial colocalization with the clusters induced by Net1 (arrowheads). The arrow indicates a Cajal body colocalizing with a Net1 cluster. Bar = 10 μm in all panels.

However, there were never more than six Cajal bodies per cell and we observed up to 80 Dlg clusters in a single cell, suggesting that most Net1-PDZ protein clusters were not Cajal bodies. However, it has been shown that one of the Cajal bodies is always associated with PML bodies, suggesting that the limited colocalization observed may not be coincidental (21).

Deletion of the NLS in Net1 prevents nuclear cluster formation. There are two alternatively spliced variants of Net1: Net1 and Net1A. Net1A is identical to Net1 except for its amino terminus, which is approximately 60 amino acids shorter (Fig. 6A). It has been previously shown that the information required to target both Net1 isoforms to the nucleus is encoded at their N termini and that mutations in this region result in the redistribution of both proteins to the cytosol (42, 49, 55). There are at least four patches of basic amino acids at the N terminus of Net1 that have been recognized as important for targeting it to the nucleus (Fig. 6A) (42, 49, 55). We have observed that both Net1 and Net1A were indistinguishable in their ability to translocate Dlg proteins to the nucleus (Fig. 2).

Net1 lacking its N terminus (oncoNet1) (Fig. 6A) has been shown to be transforming in NIH 3T3 cells (2, 8, 49). To determine whether oncoNet1 interacted with its PDZ-binding partners in a manner analogous to that of its wild-type counterparts, we generated a similar deletion mutant (ΔN) (Fig. 6A) and coexpressed it with PSD95, Dlg1, or SAP102 in HeLa cells. As previously described, while the ΔN mutant was still able to target to the nucleus to a small extent, the majority of the protein localized to the cytosol (Fig. 6B) (49, 55). Surprisingly, when Net1ΔN was coexpressed with the PDZ proteins, the PDZ protein clusters are still formed, but they were completely excluded from the nucleus and instead distributed evenly throughout the cytosol (Fig. 6C). The cytosolic clusters did not appear to contain Net1ΔN, as judged by the myc staining. However, when we repeated the experiment using an mCherry-labeled Net1ΔN mutant, we observed perfect colocalization, suggesting that the inability to see Net1ΔN in the cytosolic clusters was attributable to a lack of accessibility of the myc epitope (see Fig. S1 in the supplemental material). We also observed that the formation of these cytosolic clusters was abrogated by deleting the PDZ-binding site in Net1ΔN, indicating the requirement for interaction between Net1 and PDZ-binding proteins for cluster formation (shown for SAP102 cotransfection in Fig. 6D). These data also indicate that nuclear localization is not a requisite for these coclusters to form.

Endogenous Dlg1 localization is affected by overexpression of Net1 or by reduction of endogenous Net1 levels. We also wanted to determine if overexpression of Net1 or Net1 mutants was able to affect the localization of endogenous Dlg1. We therefore transfected MCF10a cells, which express endogenous Dlg1, with different Net1 constructs and analyzed Dlg1 localization by immunofluorescence. Figure 7A shows that overexpression of full-length Net1 promoted the translocation of Dlg1 from cell junctions to the nucleus. In many cases, we found Dlg1 colocalizing with Net1 in nuclear subdomains similar to those observed in the cotransfection experiments. The relocation of Dlg1 was completely abolished when we overexpressed Net1Δ4, which is still targeted to the nucleus but is unable to bind Dlg1, suggesting that it is being mediated by the

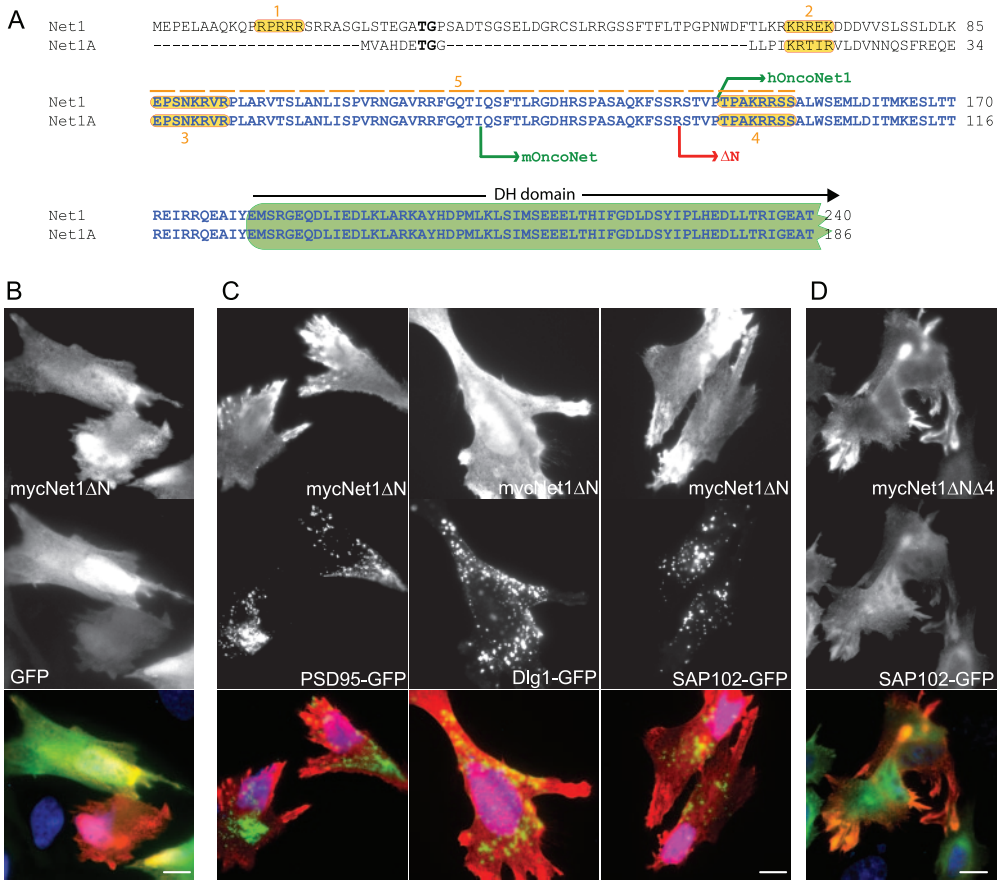

FIG. 6. (A) N-terminal domains of Net1 and Net1A. The oncogenic mutants and deletion mutants used in this study are indicated. NLS are shaded in orange and were previously characterized in references 55 (regions 1 and 2), 42 (regions 3 and 4), and 49 (region 5). (B) Overexpression of mycNet1ΔN. Net1ΔN localizes to the nucleus and to the cytosol. (C) Single and double transfections were performed with HeLa cells, combining mycNet1ΔN with either GFP-PSD95, GFP-Dlg1, or GFP-SAP102. The cells were then fixed and processed for immunofluorescence using anti-myc antibodies (red) and analyzed also for the GFP signal (green). Deletion of the NLS in Net1 inhibits the formation of nuclear subdomains. The two proteins are still able to cocluster in the cytosol. (D) Deletion of the PDZ-binding motif in Net1ΔN (Net1ΔNΔ4) abolishes the relocalization and clustering of the Dlg proteins in the cytosol (shown for SAP102). Bar = 10 μm in all panels.

interaction between the PDZ domains in Dlg1 and the PDZ-binding tail in Net1 (Fig. 7B). XPLN, another RhoA GEF that also binds PDZ proteins, is unable to relocate Dlg1 upon overexpression, suggesting that the effect observed is specific for Net1 (Fig. 7C). In addition, Net1ΔN, which is mostly cytosolic, also promotes the relocation of endogenous Dlg1, this time from cell junctions to a diffuse cytosolic pattern. In some cells, we observed cytosolic clusters similar to the ones shown in Fig. 6 (Fig. 7D). It appears in some of the images in Fig. 7 that only the transfected cells are expressing Dlg1. There are two main reasons for this apparent anomaly. First, methanol fixation, which is required to visualize nuclear Dlg1, significantly decreases the Dlg1 signal at the membranes. Second, the signal of nuclear Dlg1 in transfected cells is highly concentrated in a small area, making it difficult for the camera to capture the weaker signal at the junctions. Overall, it appears that the junctional staining is reduced and nuclear staining (or cytosolic staining in the case of ΔN) is greatly increased in transfected cells, while in reality, Dlg1 relocates only upon transfection and the difference observed is caused by the reduction in junctional staining resulting from the methanol fixation (see Fig. S2 in the supplemental material). We also tested the stability of Dlg1 upon Net1 transfection to see if Net1 overexpression could confer stability to Dlg1 and cause its accumulation over time. We transfected cells with different amounts of Net1 or Net1ΔN and then blotted for Dlg1 to see if we could detect an increase in Dlg1 levels in transfected cells. Our results showed that Net1 or Net1ΔN failed to increase Dlg1 stability and, under at least one condition, even caused a slight decrease in Dlg1 levels. These results suggest that the stability of Dlg1 is not responsible for the apparent accumulation observed in transfected cells (see Fig. S2C and E in the supplemental material).

To determine if endogenous Net1 was playing a role in targeting Dlg1 to the nucleus, we first decided to address whether we were able to detect endogenous Dlg1 in nuclear fractions. Detection of nuclear Dlg1 by immunofluorescence has already been reported (39, 40). We were also able to detect Dlg1 in the nucleus in certain cell lines, including MCF7, especially when they are not polarized (Fig. 7E). In addition, we analyzed for the presence of endogenous Dlg1 in the nucleus by using subcellular fractionation. We optimized a pro-

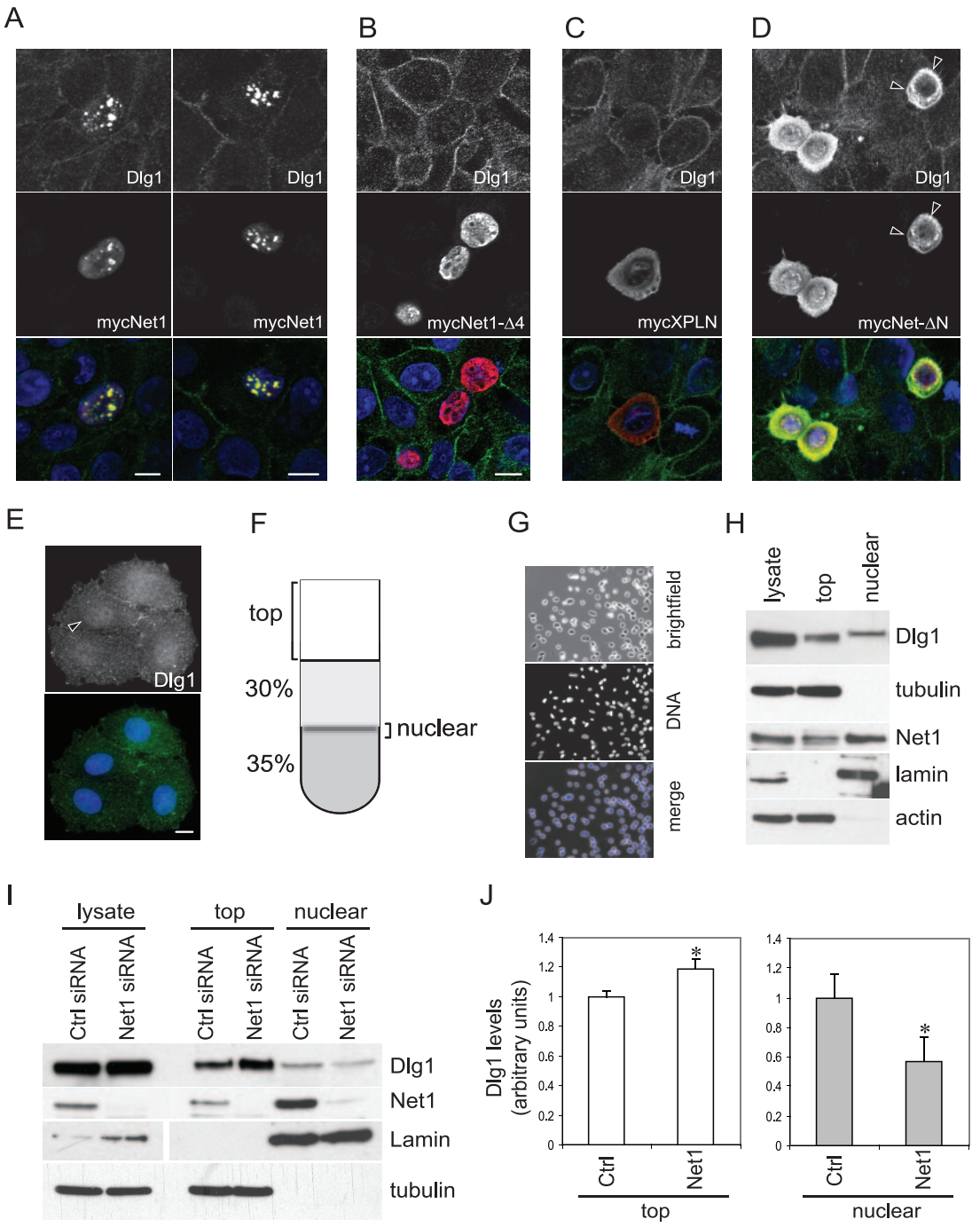

FIG. 7. MCF10a cells were transfected with the indicated constructs and processed for immunofluorescence, using anti-myc antibodies (red) to detect transfected cells, and analyzed also for endogenous Dlg1 by using anti-Dlg1 antibodies (green). Nuclear DNA was stained with Hoechst (blue). (A) Expression of Net1 promotes the redistribution of endogenous Dlg1 from the cell junctions to the nucleus (two representative cells are shown). (B) Deletion of the last four amino acids in Net1 (Net1Δ4) inhibits Dlg1 recruitment to the nucleus. (C) Expression of Net1's closest homologue, XPLN, has no effect in the localization of endogenous Dlg1. (D) Expression of the oncogenic Net1 protein (Net1ΔN) promotes the redistribution of endogenous Dlg1 from cell junctions to a diffuse cytosolic localization. Arrowheads indicate cytosolic clusters containing Dlg1 and Net1ΔN. (E) MCF7 cells were plated on coverslips and processed for immunofluorescence using anti-Dlg1 antibodies. The arrowhead indicates nuclear Dlg1. (F) Schematics of the discontinuous gradient utilized to isolate nuclei. Nucleus sediment in the 30 to 35% iodixanol interface is shown. The majority of the soluble proteins are recovered in the top fraction. (G) Representative image of a nuclear fraction. Nuclei were mixed 1:1 in mounting solution containing Hoechst to stain DNA. (H) Characterization of isolated nuclei. Proteins were separated by SDS-PAGE and immunoblotted for Dlg1, Net1, tubulin, lamin, and actin. (I) HEK293 cells were transfected with siRNA specific for Net1 or a nontargeting control siRNA. Ninety-six hours after transfection, nuclei were isolated as described in Materials and Methods. Equal amounts of protein from each fraction were then separated by SDS-PAGE and immunoblotted for Dlg1 and Net1. Membranes were stripped and reblotted for tubulin and lamin as loading controls for the top and nuclear fractions, respectively. Nuclear Dlg1 decreases when Net1 levels are reduced by siRNA treatment. (J) The amount of Dlg1 in each fraction was quantified by densitometric analysis. Values were normalized in relation to the control (ctrl) condition for each fraction. The results from three independent experiments were analyzed. Error bars represent standard errors of the means. Significance of difference from the control was estimated by Student's *t* test for paired values. Values that are significantly different from the control are marked with an asterisk. $P = 0.0348$ for the top fraction; $P = 0.0033$ for the nuclear fraction. Bar = 10 μm in all panels.

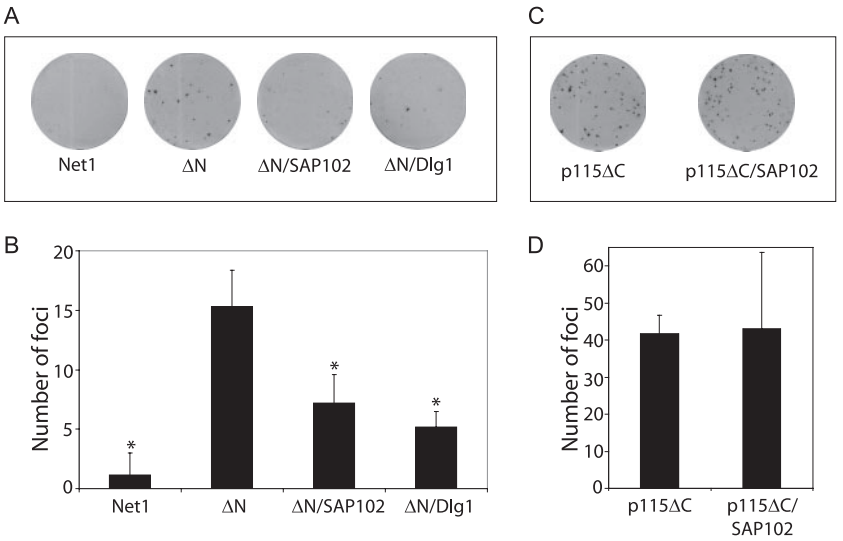

FIG. 8. (A, C) Representative focus formation assay in NIH 3T3 cells. NIH 3T3 cells were transfected with the indicated constructs and analyzed for the formation of foci. (B, D) The data shown are representative of two independent experiments performed in triplicate and represent average numbers of foci generated. Error bars represent standard deviations. Significance of difference from the control (ΔN in panel B, p115ΔC in panel D) was estimated by Student's *t* test for nonpaired values. Bars not significantly different from the control values were left unmarked. An asterisk signifies a *P* value of <0.001.

tocol that uses a discontinuous gradient of iodixanol (OptiPrep) and allows for the purification of intact nuclei in a relatively simple approach. A schematic of the gradient utilized and the fractions analyzed is depicted in Fig. 7F, and a representative microscopic image of a typical nuclear fraction is shown in Fig. 7G. Western blot analysis of the gradient fractions shows that the nuclear envelope protein lamin is found exclusively in the nuclear fraction, while soluble proteins like tubulin and actin are almost exclusively found in the soluble (top) fraction (Fig. 7H). Endogenous Net1, as expected, was highly enriched in the nuclear fractions. Interestingly, while the majority of Dlg1 can be found in the soluble (top) fraction, a significant amount of Dlg1 was consistently found in the nuclear fractions. We estimated the amount of Dlg1 in the nuclear fraction to be approximately 2 to 4% of the total Dlg1 protein. We then wanted to determine if the localization of Dlg1 in the nucleus was mediated by Net1. If Net1 is involved in targeting Dlg1 to the nucleus, then specific knockdown of Net1 should release Dlg1 from the nucleus. To address this question, we transfected cells with a Net1-specific siRNA oligonucleotide or with a control nontargeting siRNA and then prepared nuclei as described above and analyzed them for the presence of Dlg1 in the different fractions. As shown in Fig. 7I, Net1 levels were efficiently reduced by the siRNA oligonucleotide but not under the control condition. Following fractionation, we observed a redistribution of Dlg1 levels between the nuclear and the soluble fractions. The reduction of Net1 levels caused a statistically significant reduction in the levels of nuclear Dlg1 and a concomitant increase in the soluble Dlg1 levels (Fig. 7I and J), suggesting that nuclear Dlg1 is being released to the cytosol upon Net1 depletion. The fact that Dlg1 reduction was not complete can be attributed in part to residual levels of Net1 in the nucleus. Alternatively, other PDZ-binding proteins or binding partners may be contributing to the shuttling or retention of some Dlg1 in the nucleus. In summary, our results suggest that endogenous Dlg1 is found in the nucleus and that Net1 plays a role in its nuclear localization.

Role of Net1 interaction with PDZ proteins in transformation. The observation that coexpression of the oncogenic Net1ΔN mutant with PDZ domain proteins caused the formation of clusters in the cytosol suggests that Net1ΔN may sequester these proteins from their natural partners/effectors and prevent them from performing their normal function. Interestingly, Dlg1/SAP97 has been shown to function as a tumor suppressor protein in *Drosophila* and in mammals (20, 45, 64, 69–71). In addition, a mutant of Net1ΔN lacking its PDZ-binding motif loses its transformation potential, suggesting that binding to a PDZ protein is required for transformation (49). We hypothesized that the transformation ability of Net1ΔN was dependent on its ability to bind and sequester Dlg1 (or other Dlg proteins) in the cytosol, away from its normal cellular location and/or binding partners. One prediction of this hypothesis is that if we restore the amount of Dlg1 by overexpressing it, there would be enough "active" or "free" Dlg1 that can act as a tumor suppressor and reduce Net1ΔN transformation potential. To test this prediction, we coexpressed wild-type and oncogenic Net1, alone or together with Dlg1 or SAP102, in NIH 3T3 cells and performed a focus formation assay. As previously described, wild-type Net1 was unable to induce transformation while expression of Net1ΔN induced a significant increase in the number of foci formed after 2 weeks (Fig. 8A and B) (2, 49). However, when either Dlg1 or SAP102 was coexpressed with Net1ΔN, a significant reduction in the number of colonies was observed. To rule out that the observed reduction was simply a result of overexpressing a tumor suppressor, SAP102 was coexpressed with another RhoA GEF, p115-RhoGEF, which upon deletion of its C terminus is also a potent oncogene (10, 16, 68). Oncogenic p115-RhoGEF (p115ΔC) does not contain a PDZ-binding site and has not been shown to interact with SAP102 (18). Our results

show that coexpression of SAP102 with the oncogenic p115-RhoGEF had no effect on the number of foci formed after 2 weeks, suggesting that its effect on Net1ΔN-mediated transformation was specific (Fig. 8C and D).

DISCUSSION

There is now considerable evidence that aberrant function of Rho GTPases plays a significant role in cancer development. For example, constitutively active Rho mutants are capable of transforming fibroblasts and dominant-negative mutants can prevent Ras-mediated transformation (53). However, unlike for Ras, there are no reports of mutated, constitutively active forms of Rho proteins in tumors, suggesting that the mechanisms involving Rho GTPase deregulation are indirect and involve alterations in Rho GTPase expression and activation (30, 53). In contrast to Rho GTPases, Rho GEFs do acquire activating mutations, making these activators the best candidates for aberrant Rho GTPase regulation in human cancer. Many GEFs, including Dbl, Lbc, Lfc, Lsc, Dbs, Vav, Ect2, Tim, and Net1, were originally isolated as truncated oncogenes by using NIH 3T3 fibroblast transformation assays with DNA derived from various human tumors (54). These Rho GEFs are usually more potent oncogenes than their corresponding Rho GTPase mutants, suggesting that the ability to cycle between GTP- and GDP-bound states is important for Rho protein-mediated transformation.

Originally, it was thought that the ability of Net1 to transform cells was due to the fact that the ΔN mutant was constitutively active in the cytosol (55). However, it was later shown that wild-type Net1 artificially targeted to the cytosol is still active but cannot induce transformation (49). In addition, it was also shown that deletion of the last four amino acids in Net1, carrying a consensus PDZ-binding motif, abrogated its transformation properties but not its exchange activity, suggesting that binding to a PDZ protein was necessary for the process of transformation (49).

In this study, we identified several PDZ domain-containing proteins as potential binding partners for Net1 and specifically characterized the interaction of Net1 with three members of the Dlg family of proteins, PSD95, Dlg1/SAP97, and SAP102. We found that the binding of Net1 to these proteins promotes their relocation from the cytosol to discrete nuclear subdomains. This relocation requires the PDZ-binding domain and the NLS in Net1. In addition, we found that reducing Net1 levels using siRNA causes a redistribution of endogenous Dlg1 from the nucleus to the cytosol.

Although most PDZ proteins are associated with plasma membrane-bound proteins, there are several examples in the literature of PDZ proteins, including Dlg1, that are able to shuttle between the nucleus and the cytosol. For example, endogenous Dlg has been shown to localize to the nucleus in various cell types and tissues (39, 40). In this regard, Dlg1 is predicted to contain four or five putative NLS, but it is not clear which ones contribute to the nuclear localization (40). CASK, another member of the MAGUK family of proteins, has also been found to shuttle between the nucleus and the cytosol (29). CASK interacts with Tbr1, a transcription factor involved in mouse forebrain development. Once in the nucleus, CASK and Tbr-1 bind to a specific DNA sequence (the T element). In this context, CASK acts as a coactivator of Tbr-1 to induce the transcription of T-element-containing genes (29). Similarly, a splice variant of the PDZ protein NHERF2, named SIP-1, was identified as a nuclear factor binding to SRY, a Y-chromosome-specific gene that acts as a trigger for male sex development (48). SIP-1 is also proposed to function as a transcriptional coactivator (48, 63). Taken together, these studies suggest potential roles for some PDZ proteins in the nucleus, most likely associated with transcriptional regulation.

The interaction between Net1 and members of the Dlg family not only targets them to the nucleus but also localizes the complexes in discrete nuclear subdomains. The nucleus is organized into many functionally specialized subdomains that have been characterized as organelles (26, 59). Subnuclear organelles differ in size, shape, and molecular components, and the functions of most of these organelles are still unknown. Our work suggests that the structures formed by Net1 in complex with PDZ proteins are closely associated with PML bodies. PML bodies, also known as PML oncogenic domains or nuclear domain 10 (ND10), are defined by the presence of the PML protein. Approximately 10 to 30 bodies are observed in each cell, ranging from ~0.2 to 1.0 μm each. PML bodies are multiprotein complexes that have been shown to contain at least 50 different proteins (41). Studies of the physiological role of PML bodies and the PML protein have shown that they play a role in transformation suppression, growth control, differentiation, and immune response pathways (6, 41). It would be interesting to determine if the ability of Dlg1 to localize to the nucleus in close association with PML bodies is correlated to its tumor suppressor function.

Dlg1 is the mammalian homolog of the *Drosophila* discs-large (Dlg) tumor suppressor protein (38, 43). Loss of zygotic Dlg in *Drosophila* causes cellular outgrowth in larval brain and imaginal discs (20, 70, 71). Transgenic expression of mammalian Dlg1 and SAP102 can suppress tumor formation in *dlg* mutant flies and mimic Dlg at larval neuromuscular junctions, demonstrating a conservation in the tumor suppressor function (64). Dlg1 has also been shown to prevent unscheduled growth in mouse retina (45). Our data suggest that oncogenic Net1 may promote transformation by promoting the translocation of Dlg1, PSD95, and SAP102 into cytosolic clusters. This may sequester Dlg1 away from its normal localization or compete for other binding partners to promote unrestricted growth and transformation. In a similar manner, several viral oncoproteins that contain PDZ-binding tails have been shown to interact with Dlg1 and other PDZ-containing proteins (33, 34, 52). It has also been shown that the PDZ-binding motif plays a role in transformation induced by these oncoproteins (28, 34, 66). Upon interacting with Dlg1, these viral proteins inactivate the tumor suppressor protein through different molecular mechanisms. For example, the high-risk human papillomavirus E6 protein targets human Dlg1 (hDlg) and PSD95 (Dlg4) for degradation (19, 25). Significantly, only E6 proteins that are derived from oncogenic human papillomavirus types can interact with hDlg, and E6 mutants that can no longer bind hDlg also lose their transforming activity (33). In addition, E6 has been shown to colocalize at the nucleus with PML bodies (22, 23). Similarly, the viral oncoprotein Tax1, which is from human T-cell leukemia virus 1, can also bind to Dlg1 and perturb its

tumor suppression function, by a mechanism that does not involve degradation of Dlg1 (60). In contrast, the adenovirus type 9 E4-ORF1 oncoprotein induces transformation by binding to Dlg1 through a pathway that requires Src-dependent phosphatidylinositol 3-kinase activation (14). In this regard, we have not observed degradation of Dlg1 or the other PDZ proteins upon interaction with Net1, but it is possible that the cytosolic aggregation or clustering may also inhibit the tumor suppressor function of Dlg1 by preventing it from interacting with its physiological binding partners or from targeting to its appropriate cellular destination. Future experiments will be directed to characterize the molecular mechanisms by which the interaction between Net1 and PDZ proteins contributes to Net1-dependent transformation.

ACKNOWLEDGMENTS

This work was supported by NIH grants GM29860 and HL45100 to K.B. R.G.-M. was funded by a UNCF-Pfizer postdoctoral fellowship and is currently funded by a Susan Komen Foundation postdoctoral fellowship.

We thank Hal Mekeel for his assistance with electron microscopy. We thank Klaus Hahn, Mike Ehlers, and Karl Fu for providing reagents.

REFERENCES

1. **Alberts, A. S., H. Qin, H. S. Carr, and J. A. Frost.** 2005. PAK1 negatively regulates the activity of the Rho exchange factor NET1. J. Biol. Chem. **280:**12152–12161.
2. **Alberts, A. S., and R. Treisman.** 1998. Activation of RhoA and SAPK/JNK signalling pathways by the RhoA-specific exchange factor mNET1. EMBO J. **17:**4075–4085.
3. **Arthur, W. T., and K. Burridge.** 2001. RhoA inactivation by p190RhoGAP regulates cell spreading and migration by promoting membrane protrusion and polarity. Mol. Biol. Cell **12:**2711–2720.
4. **Arthur, W. T., S. M. Ellerbroek, C. J. Der, K. Burridge, and K. Wennerberg.** 2002. XPLN, a guanine nucleotide exchange factor for RhoA and RhoB, but not RhoC. J. Biol. Chem. **277:**42964–42972.
5. **Audebert, S., C. Navarro, C. Nourry, S. Chasserot-Golaz, P. Lecine, Y. Bellaiche, J. L. Dupont, R. T. Premont, C. Sempere, J. M. Strub, A. Van Dorsselaer, N. Vitale, and J. P. Borg.** 2004. Mammalian Scribble forms a tight complex with the betaPIX exchange factor. Curr. Biol. **14:**987–995.
6. **Borden, K. L.** 2002. Pondering the promyelocytic leukemia protein (PML) puzzle: possible functions for PML nuclear bodies. Mol. Cell. Biol. **22:**5259–5269.
7. **Burridge, K., and K. Wennerberg.** 2004. Rho and Rac take center stage. Cell **116:**167–179.
8. **Chan, A. M., S. Takai, K. Yamada, and T. Miki.** 1996. Isolation of a novel oncogene, NET1, from neuroepithelioma cells by expression cDNA cloning. Oncogene **12:**1259–1266.
9. **Chen, T. L., P. Y. Wang, W. Luo, S. S. Gwon, N. W. Flay, J. Zheng, C. Guo, M. L. Tanzer, and B. M. Vertel.** 2001. Aggrecan domains expected to traffic through the exocytic pathway are misdirected to the nucleus. Exp. Cell Res. **263:**224–235.
10. **Chikumi, H., A. Barac, B. Behbahani, Y. Gao, H. Teramoto, Y. Zheng, and J. S. Gutkind.** 2004. Homo- and hetero-oligomerization of PDZ-RhoGEF, LARG and p115RhoGEF by their C-terminal region regulates their in vivo Rho GEF activity and transforming potential. Oncogene **23:**233–240.
11. **Dobrosotskaya, I. Y.** 2001. Identification of mNET1 as a candidate ligand for the first PDZ domain of MAGI-1. Biochem. Biophys. Res. Commun. **283:**969–975.
12. **Fabre, S., C. Reynaud, and P. Jalinot.** 2000. Identification of functional PDZ domain binding sites in several human proteins. Mol. Biol. Rep. **27:**217–224.
13. **Fanning, A. S., and J. M. Anderson.** 1996. Protein-protein interactions: PDZ domain networks. Curr. Biol. **6:**1385–1388.
14. **Frese, K. K., I. J. Latorre, S. H. Chung, G. Caruana, A. Bernstein, S. N. Jones, L. A. Donehower, M. J. Justice, C. C. Garner, and R. T. Javier.** 2006. Oncogenic function for the Dlg1 mammalian homolog of the Drosophila discs-large tumor suppressor. EMBO J. **25:**1406–1417.
15. **Fu, L., Y. S. Gao, A. Tousson, A. Shah, T. L. Chen, B. M. Vertel, and E. Sztul.** 2005. Nuclear aggresomes form by fusion of PML-associated aggregates. Mol. Biol. Cell **16:**4905–4917.
16. **Fukuhara, S., H. Chikumi, and J. S. Gutkind.** 2001. RGS-containing RhoGEFs: the missing link between transforming G proteins and Rho? Oncogene **20:**1661–1668.
17. **Garcia-Mata, R., Z. Bebok, E. J. Sorscher, and E. S. Sztul.** 1999. Characterization and dynamics of aggresome formation by a cytosolic GFP-chimera. J. Cell Biol. **146:**1239–1254.
18. **Garcia-Mata, R., and K. Burridge.** 2007. Catching a GEF by its tail. Trends Cell Biol. **17:**36–43.
19. **Gardiol, D., C. Kuhne, B. Glaunsinger, S. S. Lee, R. Javier, and L. Banks.** 1999. Oncogenic human papillomavirus E6 proteins target the discs large tumour suppressor for proteasome-mediated degradation. Oncogene **18:**5487–5496.
20. **Goode, S., and N. Perrimon.** 1997. Inhibition of patterned cell shape change and cell invasion by Discs large during Drosophila oogenesis. Genes Dev. **11:**2532–2544.
21. **Grande, M. A., I. van der Kraan, B. van Steensel, W. Schul, H. de The, H. T. van der Voort, L. de Jong, and R. van Driel.** 1996. PML-containing nuclear bodies: their spatial distribution in relation to other nuclear components. J. Cell. Biochem. **63:**280–291.
22. **Guccione, E., K. J. Lethbridge, N. Killick, K. N. Leppard, and L. Banks.** 2004. HPV E6 proteins interact with specific PML isoforms and allow distinctions to be made between different POD structures. Oncogene **23:**4662–4672.
23. **Guccione, E., P. Massimi, A. Bernat, and L. Banks.** 2002. Comparative analysis of the intracellular location of the high- and low-risk human papillomavirus oncoproteins. Virology **293:**20–25.
24. **Hall, A.** 2005. Rho GTPases and the control of cell behaviour. Biochem. Soc. Trans. **33:**891–895.
25. **Handa, K., T. Yugawa, M. Narisawa-Saito, S. I. Ohno, M. Fujita, and T. Kiyono.** 2007. E6AP-dependent degradation of DLG4/PSD95 by high-risk human papillomavirus type 18 E6 protein. J. Virol. **81:**1379–1389.
26. **Handwerger, K. E., and J. G. Gall.** 2006. Subnuclear organelles: new insights into form and function. Trends Cell Biol. **16:**19–26.
27. **Harris, B. Z., and W. A. Lim.** 2001. Mechanism and role of PDZ domains in signaling complex assembly. J. Cell Sci. **114:**3219–3231.
28. **Hirata, A., M. Higuchi, A. Niinuma, M. Ohashi, M. Fukushi, M. Oie, T. Akiyama, Y. Tanaka, F. Gejyo, and M. Fujii.** 2004. PDZ domain-binding motif of human T-cell leukemia virus type 1 Tax oncoprotein augments the transforming activity in a rat fibroblast cell line. Virology **318:**327–336.
29. **Hsueh, Y. P., T. F. Wang, F. C. Yang, and M. Sheng.** 2000. Nuclear translocation and transcription regulation by the membrane-associated guanylate kinase CASK/LIN-2. Nature **404:**298–302.
30. **Karnoub, A. E., M. Symons, S. L. Campbell, and C. J. Der.** 2004. Molecular basis for Rho GTPase signaling specificity. Breast Cancer Res. Treat. **84:**61–71.
31. **Kim, E., M. Niethammer, A. Rothschild, Y. N. Jan, and M. Sheng.** 1995. Clustering of Shaker-type K+ channels by interaction with a family of membrane-associated guanylate kinases. Nature **378:**85–88.
32. **Kim, E., and M. Sheng.** 1996. Differential K+ channel clustering activity of PSD-95 and SAP97, two related membrane-associated putative guanylate kinases. Neuropharmacology **35:**993–1000.
33. **Kiyono, T., A. Hiraiwa, M. Fujita, Y. Hayashi, T. Akiyama, and M. Ishibashi.** 1997. Binding of high-risk human papillomavirus E6 oncoproteins to the human homologue of the Drosophila discs large tumor suppressor protein. Proc. Natl. Acad. Sci. USA **94:**11612–11616.
34. **Lee, S. S., R. S. Weiss, and R. T. Javier.** 1997. Binding of human virus oncoproteins to hDlg/SAP97, a mammalian homolog of the Drosophila discs large tumor suppressor protein. Proc. Natl. Acad. Sci. USA **94:**6670–6675.
35. **Link, C. D., V. Fonte, B. Hiester, J. Yerg, J. Ferguson, S. Csontos, M. A. Silverman, and G. H. Stein.** 2006. Conversion of green fluorescent protein into a toxic, aggregation-prone protein by C-terminal addition of a short peptide. J. Biol. Chem. **281:**1808–1816.
36. **Liu, B. P., and K. Burridge.** 2000. Vav2 activates Rac1, Cdc42, and RhoA downstream from growth factor receptors but not beta1 integrins. Mol. Cell. Biol. **20:**7160–7169.
37. **Liu, M., and A. Horowitz.** 2006. A PDZ-binding motif as a critical determinant of Rho guanine exchange factor function and cell phenotype. Mol. Biol. Cell **17:**1880–1887.
38. **Lue, R. A., S. M. Marfatia, D. Branton, and A. H. Chishti.** 1994. Cloning and characterization of hdlg: the human homologue of the Drosophila discs large tumor suppressor binds to protein 4.1. Proc. Natl. Acad. Sci. USA **91:**9818–9822.
39. **Mantovani, F., and L. Banks.** 2003. Regulation of the discs large tumor suppressor by a phosphorylation-dependent interaction with the beta-TrCP ubiquitin ligase receptor. J. Biol. Chem. **278:**42477–42486.
40. **McLaughlin, M., R. Hale, D. Ellston, S. Gaudet, R. A. Lue, and A. Viel.** 2002. The distribution and function of alternatively spliced insertions in hDlg. J. Biol. Chem. **277:**6406–6412.
41. **Melnick, A., and J. D. Licht.** 1999. Deconstructing a disease: RARalpha, its fusion partners, and their roles in the pathogenesis of acute promyelocytic leukemia. Blood **93:**3167–3215.
42. **Miyakoshi, A., N. Ueno, and N. Kinoshita.** 2004. Rho guanine nucleotide exchange factor xNET1 implicated in gastrulation movements during Xenopus development. Differentiation **72:**48–55.
43. **Muller, B. M., U. Kistner, R. W. Veh, C. Cases-Langhoff, B. Becker, E. D.**

Gundelfinger, and C. C. Garner. 1995. Molecular characterization and spatial distribution of SAP97, a novel presynaptic protein homologous to SAP90 and the Drosophila discs-large tumor suppressor protein. J. Neurosci. **15:**2354–2366.
44. **Muratani, M., D. Gerlich, S. M. Janicki, M. Gebhard, R. Eils, and D. L. Spector.** 2002. Metabolic-energy-dependent movement of PML bodies within the mammalian cell nucleus. Nat. Cell Biol. **4:**106–110.
45. **Nguyen, M. M., M. L. Nguyen, G. Caruana, A. Bernstein, P. F. Lambert, and A. E. Griep.** 2003. Requirement of PDZ-containing proteins for cell cycle regulation and differentiation in the mouse lens epithelium. Mol. Cell. Biol. **23:**8970–8981.
46. **Park, E., M. Na, J. Choi, S. Kim, J. R. Lee, J. Yoon, D. Park, M. Sheng, and E. Kim.** 2003. The Shank family of postsynaptic density proteins interacts with and promotes synaptic accumulation of the beta PIX guanine nucleotide exchange factor for Rac1 and Cdc42. J. Biol. Chem. **278:**19220–19229.
47. **Penzes, P., R. C. Johnson, R. Sattler, X. Zhang, R. L. Huganir, V. Kambampati, R. E. Mains, and B. A. Eipper.** 2001. The neuronal Rho-GEF Kalirin-7 interacts with PDZ domain-containing proteins and regulates dendritic morphogenesis. Neuron **29:**229–242.
48. **Poulat, F., P. S. Barbara, M. Desclozeaux, S. Soullier, B. Moniot, N. Bonneaud, B. Boizet, and P. Berta.** 1997. The human testis determining factor SRY binds a nuclear factor containing PDZ protein interaction domains. J. Biol. Chem. **272:**7167–7172.
49. **Qin, H., H. S. Carr, X. Wu, D. Muallem, N. H. Tran, and J. A. Frost.** 2005. Characterization of the biochemical and transforming properties of the neuroepithelial transforming protein 1. J. Biol. Chem. **280:**7603–7613.
50. **Radziwill, G., R. A. Erdmann, U. Margelisch, and K. Moelling.** 2003. The Bcr kinase downregulates Ras signaling by phosphorylating AF-6 and binding to its PDZ domain. Mol. Cell. Biol. **23:**4663–4672.
51. **Rossman, K. L., C. J. Der, and J. Sondek.** 2005. GEF means go: turning on RHO GTPases with guanine nucleotide-exchange factors. Nat. Rev. Mol. Cell Biol. **6:**167–180.
52. **Rousset, R., S. Fabre, C. Desbois, F. Bantignies, and P. Jalinot.** 1998. The C-terminus of the HTLV-1 Tax oncoprotein mediates interaction with the PDZ domain of cellular proteins. Oncogene **16:**643–654.
53. **Sahai, E., and C. J. Marshall.** 2002. RHO-GTPases and cancer. Nat. Rev. Cancer **2:**133–142.
54. **Schmidt, A., and A. Hall.** 2002. Guanine nucleotide exchange factors for Rho GTPases: turning on the switch. Genes Dev. **16:**1587–1609.
55. **Schmidt, A., and A. Hall.** 2002. The Rho exchange factor Net1 is regulated by nuclear sequestration. J. Biol. Chem. **277:**14581–14588.
56. **Sheng, M., and C. Sala.** 2001. PDZ domains and the organization of supramolecular complexes. Annu. Rev. Neurosci. **24:**1–29.
57. **Skinner, P. J., B. T. Koshy, C. J. Cummings, I. A. Klement, K. Helin, A. Servadio, H. Y. Zoghbi, and H. T. Orr.** 1997. Ataxin-1 with an expanded glutamine tract alters nuclear matrix-associated structures. Nature **389:**971–974.
58. **Solski, P. A., K. Abe, and C. J. Der.** 2000. Analyses of transforming activity of Rho family activators. Methods Enzymol. **325:**425–441.
59. **Spector, D. L.** 2001. Nuclear domains. J. Cell Sci. **114:**2891–2893.
60. **Suzuki, T., Y. Ohsugi, M. Uchida-Toita, T. Akiyama, and M. Yoshida.** 1999. Tax oncoprotein of HTLV-1 binds to the human homologue of Drosophila discs large tumor suppressor protein, hDLG, and perturbs its function in cell growth control. Oncogene **18:**5967–5972.
61. **Takahashi, J., H. Fujigasaki, C. Zander, K. H. El Hachimi, G. Stevanin, A. Durr, A. S. Lebre, G. Yvert, Y. Trottier, H. de The, J. J. Hauw, C. Duyckaerts, and A. Brice.** 2002. Two populations of neuronal intranuclear inclusions in SCA7 differ in size and promyelocytic leukaemia protein content. Brain **125:**1534–1543.
62. **Tcherkezian, J., and N. Lamarche-Vane.** 2007. Current knowledge of the large RhoGAP family of proteins. Biol. Cell **99:**67–86.
63. **Thevenet, L., K. H. Albrecht, S. Malki, P. Berta, B. Boizet-Bonhoure, and F. Poulat.** 2005. NHERF2/SIP-1 interacts with mouse SRY via a different mechanism than human SRY. J. Biol. Chem. **280:**38625–38630.
64. **Thomas, U., B. Phannavong, B. Muller, C. C. Garner, and E. D. Gundelfinger.** 1997. Functional expression of rat synapse-associated proteins SAP97 and SAP102 in Drosophila dlg-1 mutants: effects on tumor suppression and synaptic bouton structure. Mech. Dev. **62:**161–174.
65. **Van Aelst, L., and C. D'Souza-Schorey.** 1997. Rho GTPases and signaling networks. Genes Dev. **11:**2295–2322.
66. **Watson, R. A., M. Thomas, L. Banks, and S. Roberts.** 2003. Activity of the human papillomavirus E6 PDZ-binding motif correlates with an enhanced morphological transformation of immortalized human keratinocytes. J. Cell Sci. **116:**4925–4934.
67. **Wennerberg, K., and C. J. Der.** 2004. Rho-family GTPases: it's not only Rac and Rho (and I like it). J. Cell Sci. **117:**1301–1312.
68. **Whitehead, I. P., R. Khosravi-Far, H. Kirk, G. Trigo-Gonzalez, C. J. Der, and R. Kay.** 1996. Expression cloning of lsc, a novel oncogene with structural similarities to the Dbl family of guanine nucleotide exchange factors. J. Biol. Chem. **271:**18643–18650.
69. **Woodhouse, E., E. Hersperger, and A. Shearn.** 1998. Growth, metastasis, and invasiveness of Drosophila tumors caused by mutations in specific tumor suppressor genes. Dev. Genes Evol. **207:**542–550.
70. **Woods, D. F., and P. J. Bryant.** 1991. The discs-large tumor suppressor gene of Drosophila encodes a guanylate kinase homolog localized at septate junctions. Cell **66:**451–464.
71. **Woods, D. F., C. Hough, D. Peel, G. Callaini, and P. J. Bryant.** 1996. Dlg protein is required for junction structure, cell polarity, and proliferation control in Drosophila epithelia. J. Cell Biol. **134:**1469–1482.
72. **Yamada, M., T. Sato, T. Shimohata, S. Hayashi, S. Igarashi, S. Tsuji, and H. Takahashi.** 2001. Interaction between neuronal intranuclear inclusions and promyelocytic leukemia protein nuclear and coiled bodies in CAG repeat diseases. Am. J. Pathol. **159:**1785–1795.